The Complexity of Neutron Star Matter: from the Liquid-Gas Phase Transition to Chiral Symmetry Breaking and Restoration - I

Constança Providência

Universidade de Coimbra, Portugal

60th Karpacz Winter School on Theoretical Physics, May 16-24, 2024

Universidade de Coimbra

CFisUC

FCT Fundação para a Ciência e a Tecnologia
MINISTÉRIO DA CIÊNCIA, TECNOLOGIA E ENSINO SUPERIOR

MAGSTARMATTER

QCD phase diagram

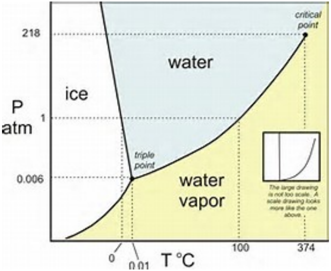

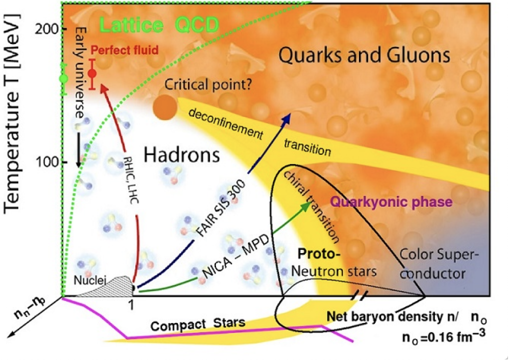

autor: Larry McLerran

Multifragmentation

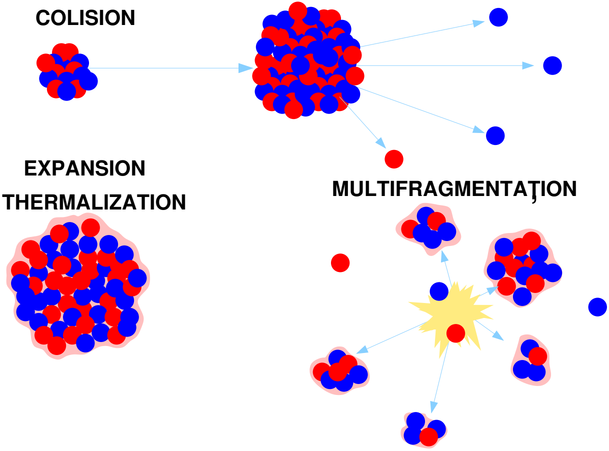

- Multifragmentation in relativistic heavy ion collisions
  - Experimental results consistent with equilibration of the excited systems prior to decay
  - This justifies a statistical and thermodynamical treatment.

Liquid-Gas Phase Transition?

Phochodzalla et *al.*, PRL75, 1995

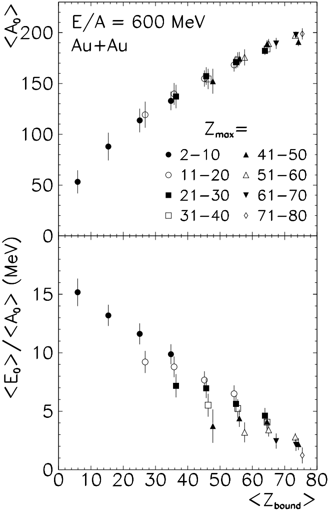

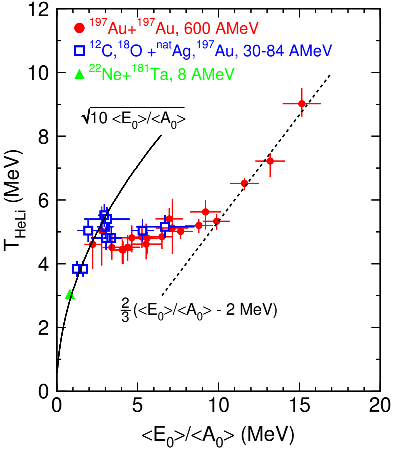

Crust

cold catalyzed matter

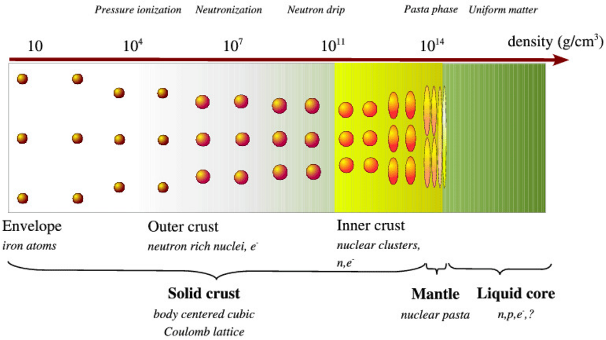

(Chamel and Haensel, Living Reviews 2008)

Nuclear Matter: Liquid-Gas Phase Transition

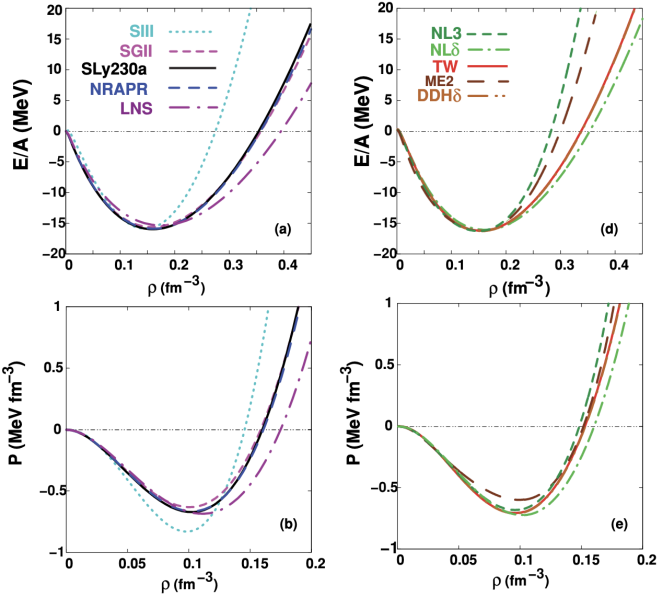

Convexity condition: one component system

Figure from Mueller & Serot PRC52,2071

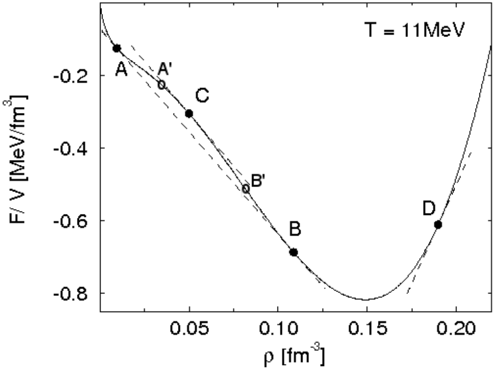

- $\mathcal{F} - \epsilon_0\rho$
- *A* and *B*: $\mathcal{F}$ is convex with common tangent (same μ)
  - coexistence of two phases with different densities
  - binodal points
- *C*: $\mathcal{F}$ is concave, the system is unstable
- *A'* and *B'*: $\partial^2\mathcal{F}/\partial\rho^2 = 0$, spinodal points

Thermodynamical instability: different models

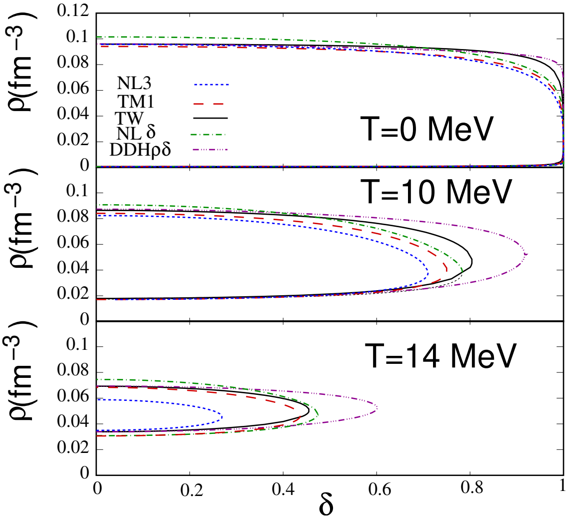

- **Largest differences:** at finite T and large δ

Nuclear Matter: Liquid-Gas Phase Transition

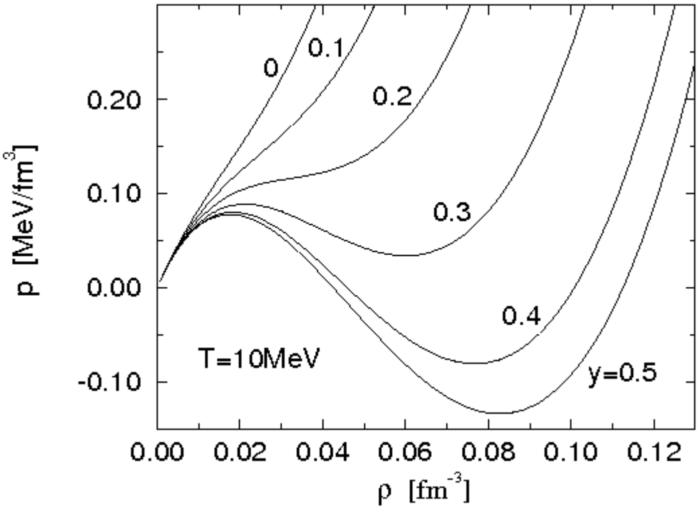

Spinodal versus Binodal

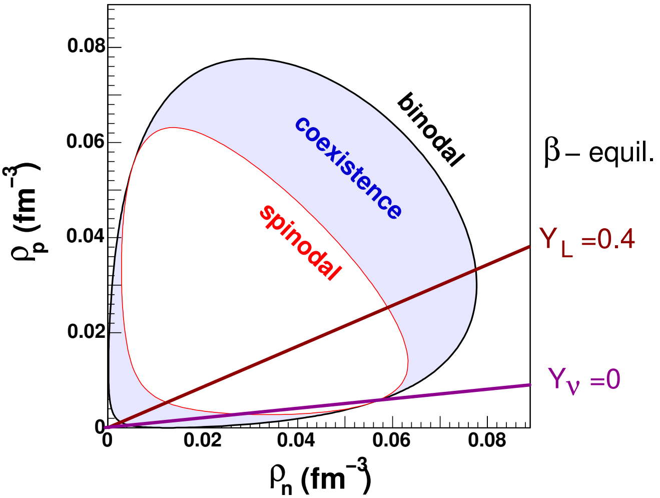

Binodal: pressure versus proton fraction

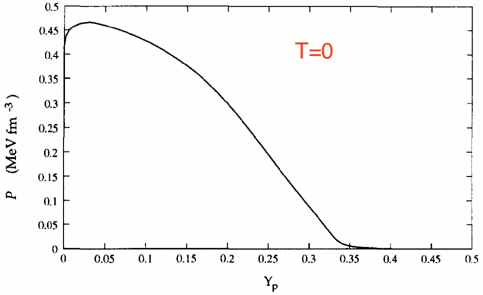

Menezes NPA650 (1999) 283

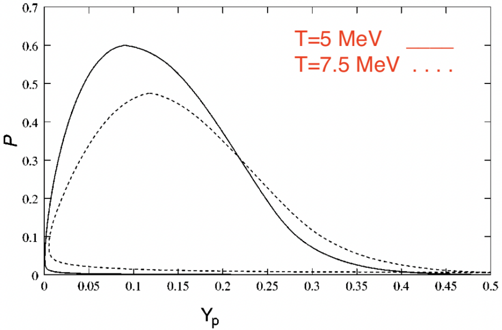

Menezes PRC60 024313 (1999)

Nuclear matter: Maxwell construction

Figure from Mueller & Serot PRC52,2071

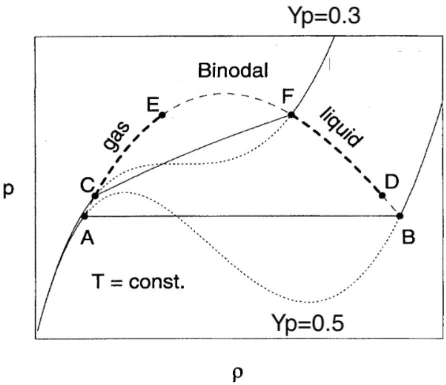

- symmetric matter ($y_p = 0.5$): $p_A = p_B$
- asymmetric matter ($y_p = 0.3$): transition occurs along the line CF, keeping $y_p = 0.3$
- Between C and F: the gas and liquid phases evolve along the binodal line

EOS: relativistic mean field description

RMF Lagrangian for stellar matter

- **Lagrangian density:** causal Lorentz-covariant Lagrangian (baryon densities and meson fields)

$$\mathcal{L}_{NLWM} = \sum_{B=baryons} \mathcal{L}_B + \mathcal{L}_{mesons} + \mathcal{L}_l + \mathcal{L}_\gamma,$$

- **Baryonic contribution:** $\mathcal{L}_B = \bar{\psi}_B \left[\gamma_\mu D_B^\mu - M_B^*\right] \psi_B,$
  $D_B^\mu = i\partial^\mu - g_{\omega B}\omega^\mu - \frac{g_{\rho B}}{2}\boldsymbol{\tau} \cdot \mathbf{b}^\mu$
  $M_B^* = M_B - g_{\sigma B}\sigma$

- **Meson contribution**

$$\mathcal{L}_{mesons} = \mathcal{L}_\sigma + \mathcal{L}_\omega + \mathcal{L}_\rho + \mathcal{L}_{non-linear}$$

- **Lepton contribution: homogeneous matter**
  $\mathcal{L}_l = \sum_l \bar{\psi}_l \left[\gamma_\mu i\partial^\mu - m_l\right] \psi_l$

- **Electromagnetic contribution:** $\mathcal{L}_\gamma = -\frac{1}{4} F_{\mu\nu} F^{\mu\nu}$

- **Electron contribution:** $\mathcal{L}_e = \bar{\psi}_e \left[\gamma_\mu \left(i\partial^\mu + eA^\mu\right) - m_e\right] \psi_e$

EOS: relativistic mean field description

Density dependence of the EOS determined by introducing

- non-linear meson terms (Boguta&Bodmer 1977, Mueller&Serot 1996)
- NL3, NL3$\omega\rho$, TM1, TM1$\omega\rho$, FSU, FSU2, FSU2R

$$\mathcal{L}_{non-linear} = -\frac{1}{3} b g_\sigma^3 (\sigma)^3 - \frac{1}{4} c g_\sigma^4 (\sigma)^4 + \frac{\xi}{4!} (g_\omega \omega_\mu \omega^\mu)^4 + \Lambda_\omega g_\varrho^2 \boldsymbol{\varrho}_\mu \cdot \boldsymbol{\varrho}^\mu g_\omega^2 \omega_\mu \omega^\mu,$$

  - Parameters: $g_i (i = \sigma, \omega, \rho)$, b, c, ξ, Λ_ω (Malik arxiv:2301.08169)

- Bayesian estimation of model parameters

EOS

RMF Lagrangian for npeμ matter

From RMF stress-energy tensor calculate energy density & pressure

$$T^{\mu\nu}_{\mathrm{RMF}} = \sum_{i=n,p,e,\mu} i\bar{\psi}_i\gamma^\mu\partial^\nu\psi_i - \eta^{\mu\nu}\mathcal{L}_{\mathrm{mesons}}$$

Energy density:

$$\epsilon = \langle T^{00}\rangle = \sum_i \langle\bar{\psi}_i\gamma_0 k_0\psi_i\rangle - \mathcal{L}_{\mathrm{mesons}}$$

Pressure

$$p = \frac{1}{3}\langle T^{ii}\rangle = \frac{1}{3}\sum_i \langle\bar{\psi}_i\gamma\cdot k\psi_i\rangle + \mathcal{L}_{\mathrm{mesons}}$$

The particle energy spectrum is

$$E_{I_3}(k) = \sqrt{{M^*}^2 + k^2} + g_\omega\omega_0 + \frac{g_\rho}{2} I_3\rho_{30}.$$

Field equations: minimize ϵ with respect to the fields

$$\frac{\partial\epsilon}{\partial\sigma} = 0, \quad \frac{\partial\epsilon}{\partial\omega_0} = 0, \quad \frac{\partial\epsilon}{\partial\rho_{30}} = 0$$

Spanning the full range of NS properties with a microscopic model

Malik ApJ930 17, Malik arxiv: 2301.08169

Constraints				
Quantity		Value/Band	Ref	DDB
NMP (MeV)	ρ_0	0.153 ± 0.005	Typel & Wolter (1999)	✓
	ϵ_0	-16.1 ± 0.2	Dutra et al. (2014)	✓
	K_0	230 ± 40	Todd-Rutel & Piekarewicz (2005); Shlomo et al. (2006)	✓
	$J_{\mathrm{sym},0}$	32.5 ± 1.8	Essick et al. (2021a)	✓
PNM (MeV fm^{-3})	$P(\rho)$	$2 \times \mathrm{N}^3\mathrm{LO}$	Hebeler et al. (2013)	✓
NS mass ($M_\odot$)	$M_{\max}$	>2.0	Fonseca et al. (2021)	✓

NS properties: full posterior NL

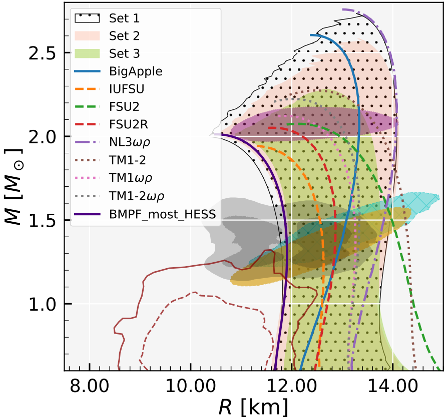

- **Observations:** GW170817, NICER J0740 and J0030, HESS
- **RMF models:** NL3$\omega\rho$,FSU2, FSU2R, IUFSU, BigApple, TM1-2($\omega\rho$)
- **Bayesian study**: Set 1 ($\xi < 0.004$), 2, 3 ($\xi > 0.015$)

Dynamical instabilities: small fluctuations

The Vlasov Equation

- Nucleons described by the distribution functions $f_i(\mathbf{p}, \mathbf{r}, t)$
- Equilibrium state of matter

$$\{f_{oi}, h_i\} = 0$$

- The time evolution of f_i is described by the Vlasov equation

$$\begin{aligned} \frac{df_i}{dt} &= 0, \qquad i = p,\ n,\ e \\ \frac{\partial f_i}{\partial t} + \{f_i, h_i\} &= 0, \end{aligned}$$

(first order of the TDHF equation in a Wigner-Kirkwood expansion)

- Single particle hamiltonian h_i (eigenstates Dirac equation)

$$h_i = \sqrt{\left(\mathbf{p} - \vec{\mathcal{V}}\right)^2 + (m - g_s\sigma)^2} + \mathcal{V}_0$$

Equilibrium State of *npe* Matter

- Equilibrium state characterized by: P_{Fn}, P_{Fp}, P_{Fe}

$$f_0(\mathbf{r},\mathbf{p}) = \mathrm{diag}\left(\Theta(P_{Fp}^2 - p^2), \Theta(P_{Fn}^2 - p^2), \Theta(P_{Fe}^2 - p^2)\right)$$

$$h_{0i} = \sqrt{\mathbf{p}^2 + \left(m - g_s\sigma^{(0)}\right)^2} + \mathcal{V}^{(0)}$$

- Charge neutrality: $P_{Fe} = P_{Fp}$
- Equilibrium fields

$$\begin{aligned}
m_s^2\phi_0 + \frac{\kappa}{2}\phi_0^2 + \frac{\lambda}{6}\phi_0^3 &= g_s\rho_s^{(0)} \\
m_v^2 V_0^{(0)} &= g_v(\rho_p + \rho_n)\ , \quad V_i^{(0)} = 0 \\
m_\rho^2 b_0^{(0)} &= \frac{g_\rho}{2}(\rho_p - \rho_n)\ , \quad b_i^{(0)} = 0 \\
A_0^{(0)} &= 0\ , \quad A_i^{(0)} = 0\ .
\end{aligned}$$

Small perturbation of the system

- Perturbed fields:

$$\phi = \phi_0 + \delta\phi\,, \quad V_0 = V_0^{(0)} + \delta V_0\,, \quad V_i = \delta V_i\,, \quad b_0 = b_0^{(0)} + \delta b_0\,, \quad b_i$$

$$A_0 = \delta A_0\,, \quad A_i = \delta A_i.$$

- Perturbed distribution function:

$$f = f_0 + \delta f\,,$$

$$\delta f_i = \{S_i, f_{0i}\}$$

- Generating function: $S(\mathbf{r}, \mathbf{p}, t) = \mathrm{diag}\left(S_p,\ S_n,\ S_e\right)\,,$

Linearized Equations of Motion

- The time evolution of f_i is described by the Vlasov equation

$$\frac{df_i}{dt} = 0, \qquad \rightarrow \frac{\partial f_i}{\partial t} + \{f_i, h_i\} = 0, \qquad i = p,\ n,\ e$$

- The linearized relativistic Vlasov equation

$$\frac{d\mathcal{S}_i}{dt} + \{\mathcal{S}_i, h_{0i}\} = \delta h_i$$

- Longitudinal fluctuations:

$$\begin{pmatrix} S_i & \delta F_j & \delta\rho_i & \delta h_i \end{pmatrix} = \begin{pmatrix} S_{\omega,i}(x) & \delta F_{\omega,j} & \delta\rho_{\omega,i} & \delta h_{\omega,i} \end{pmatrix} e^{i(\mathbf{q}\cdot\mathbf{r}-\omega t)}$$

$x = \cos(\mathbf{p}\cdot\mathbf{q})$,
$i = e, p, n$,
$j = \sigma, \omega, \rho, \gamma$

Linearized Equations of Motion

- One-body hamiltonian variation
  - Electrons

$$\delta h_e = -e\left[\delta A_0 - \frac{\mathbf{p}\cdot\delta\mathbf{A}}{\epsilon_{0e}}\right],$$

  - nucleons: relativistic models

$$\delta h_i = -g_s\delta\phi\frac{M^*}{\epsilon_0} + \delta\mathcal{V}_{0i} - \frac{\mathbf{p}\cdot\delta\boldsymbol{\mathcal{V}}_i}{\epsilon_0}, \quad i = p, n$$

Dispersion relations

- In terms of the transition densities: $\delta\rho_i = \frac{3}{2}\frac{k}{P_{Fi}}\rho_{0i}A_{\omega i}$,

$$\begin{pmatrix} 1 + F^{pp}L_p & F^{pn}L_p & C_A^{pe}L_p \\ F^{np}L_n & 1 + F^{nn}L_n & 0 \\ C_A^{ep}L_e & 0 & 1 - C_A^{ee}L_e \end{pmatrix} \begin{pmatrix} A_{\omega p} \\ A_{\omega n} \\ A_{\omega e} \end{pmatrix} = 0,$$

- Lindhard function, speed of sound:
$L(s_i) = 2 - s_i \ln\left(\frac{s_i+1}{s_i-1}\right)$, with $(s_i = \omega/\omega_{oi} = \omega/(k\,V_{Fi}))$, $V_{F_i} = \frac{P_{F_i}}{\epsilon_{F_i}}$
$F^{ij} = C_s^{ij} - C_v^{ij} - \tau_i\tau_j\,C_\rho^{ij} - C_A^{ij}\delta_{ip}\delta_{jp}, \quad i,j = n,p,$
- dispersion relation

$$[1 - C_A^{ee}L_e]\left[1 + L_pF^{pp} + L_nF^{nn} + L_pL_n\left(F^{pp}F^{nn} - F^{pn}F^{np}\right)\right]$$
$$-C_A^{ep}C_A^{pe}L_eL_p(1 + L_nF^{nn}) = 0.$$

- Surface $\omega = 0$: defines dynamical spinodal

Dynamical Spinodal

Dynamical versus thermodynamical Spinodal

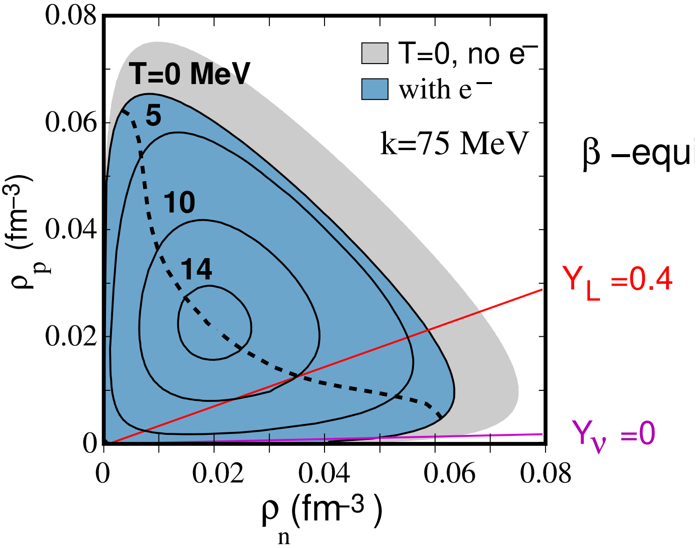

Crust

cold catalyzed matter

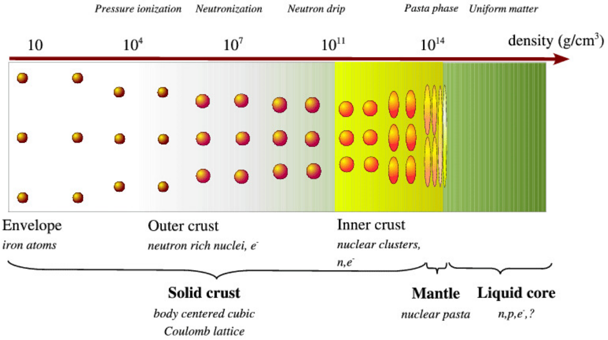

(Chamel and Haensel, Living Reviews 2008)

- Surface on NS: $p = 0$
- Lowest energy state of hadronic matter at zero compression and T: ^{56}Fe
  - surface is formed by solid iron

Inner crust - Pasta phase

No hyperons

- Inner crust:
  neutron drip density $< \ \rho \ <$ crust-core transition
  $\sim 0.003 \text{ fm}^{-3} < \ \rho \ < \sim 0.08 - 0.1 \text{ fm}^{-3}$
- a lattice of heavy and neutron-rich nuclei immersed in a sea of superfluid neutrons and ultrarelativistic electrons
- "pasta" phase: frustrated system that arises in the competition between the strong and the electromagnetic interactions
- The short- and large-distance scales related to the nuclear and Coulomb interactions are comparable at densities of the order of 10^{13} - 10^{14} g/cm^3

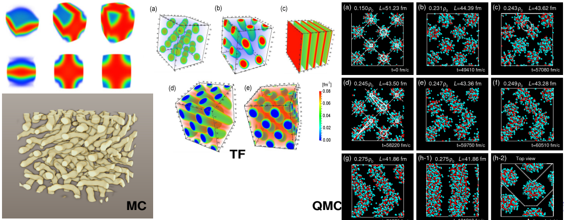

Inner crust

EOS for the inner crust:

- Bethe, Baym, Pethick (BBP): Compressible Liquid Drop Model
- Negele & Vautherin (NV):HF calculation for spherical clusters (NPA207, 1973)
- Shen, Toki, H. Shen, Toki, Oyamatsu, Sumiyoshi(STOS), Thomas-Fermi calculation within TM1, (NPA637,1998)
- Douchin & Haensel: Compressible Liquid Drop Model and Sly4 (only spherical) (AA380,2001)
- Grill *et al* : Inner crust EOS within Thomas Fermi calculation of pasta (PRC85,2012)

  NL3, TM1, GM1, DDME2,DDHδ,NL3$\omega\rho$

Pasta phase EOS

- β-equilibrium non-homgeneous matter within a TF calculation
- assumed a preferred single geometry (least free energy) for a given T, ρ and y_p
- only five possible shapes are considered: droplets, rods, slabs, tubes and bubbles
- β-equilibrium: y_P is very small and only three shapes are energetically favorable: droplets, rods and slabs.
- a regular lattice in the Wigner-Seitz approximation is considered, the WS cell having the shape of the clusters
- a fixed Z and N number at a given density determines the WS volume,
- β-equilibrium condition determines N (number of neutrons

Pasta versus homogeneous NL3 EOS

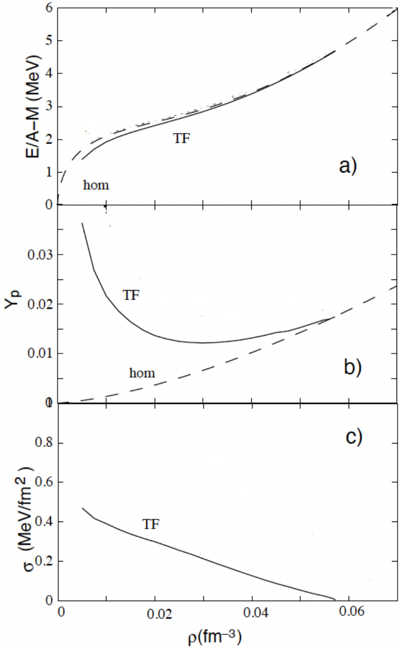

Pasta phase: Coexisting phases approximation

PRC 91, 055801 2015

- Separated regions of high (pasta phases) and low (gas) densities
- Gibbs equilibrium conditions ($T^I = T^{II}$)

$$\begin{aligned} P^I &= P^{II}, \\ \mu_i^I &= \mu_i^{II}, \quad i = p, n \end{aligned}$$

- Finite size effects, a surface and a Coulomb terms, included *a posteriori* after the coexisting phases are achieved.
- Charge neutrality: $\rho_e = Y_p \rho_B$ (uniform)
- total free energy density and total proton fraction:

$$\begin{aligned} \mathcal{F} &= f\mathcal{F}^I + (1-f)\mathcal{F}^{II} + \mathcal{F}_e + \epsilon_{surf} + \epsilon_{Coul}, \\ \rho_p &= Y_p \rho_B = f\rho_p^I + (1-f)\rho_p^{II}, \\ \rho_B &= = f\rho^I + (1-f)\rho^{II}, \end{aligned}$$

- Minimization with respect to the size of the droplet/bubble, rod/tube or slab: $\epsilon_{surf} = 2\epsilon_{Coul}$,

Pasta phase: Compressible liquid drop model

PRC 91, 055801 2015

- The total free energy density is minimized, including the surface and Coulomb terms.
- Gibbs equilibrium conditions ($T^I = T^{II}$)

$$
\begin{aligned}
\mu_n^I &= \mu_n^{II} \\
\mu_p^I &= \mu_p^{II} - \frac{\varepsilon_{surf}}{f(1-f)(\rho_p^I - \rho_p^{II})} \\
P^I &= P^{II} - \varepsilon_{surf}\left(\frac{1}{2\alpha} + \frac{1}{2\Phi}\frac{\partial\Phi}{\partial f} - \frac{\rho_p^{II}}{f(1-f)(\rho_p^I - \rho_p^{II})}\right)
\end{aligned}
$$

Pasta phase: Thomas Fermi

Self-consistent solution:

1. Initial guess for the fields
2. chemical potentials and densities are computed

$$\mu_p = \sqrt{k_{Fp}^2 + M^{*2}} + g_v \omega_0 + \frac{g_\rho}{2} b_0 + e A_0$$
$$\mu_n = \sqrt{k_{Fn}^2 + M^{*2}} + g_v \omega_0 - \frac{g_\rho}{2} b_0$$

3. new fields: solutions of the field equations

$$\nabla^2 \sigma = m_s^2 \sigma + \frac{1}{2}\kappa \sigma^2 + \frac{1}{3!}\lambda \sigma^3 - g_s \rho_s,$$
$$\nabla^2 \omega_0 = m_v^2 \omega_0 + \frac{\xi g_v^4}{6}\omega_0^3 - g_v \rho_B,$$
$$\nabla^2 b_0 = m_\rho^2 b_0 - \frac{g_\rho}{2}\rho_3,$$
$$\nabla^2 A_0 = -e\rho_p$$

4. return to (2)

repeat for several geometries

Crust-core transition

Pasta (TF) versus dynamical and thermodynamical spinodals, T=0

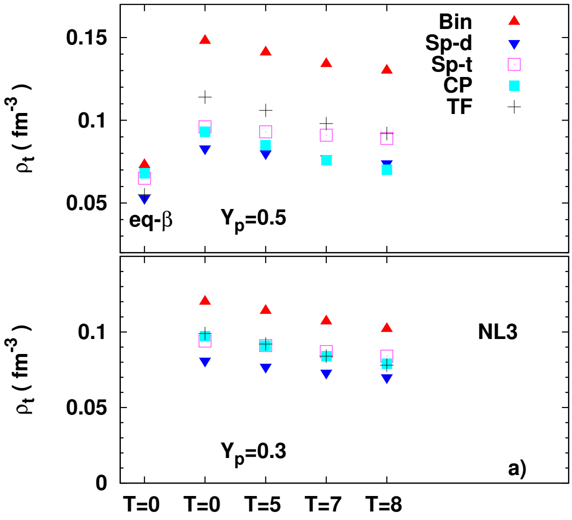

(Avancini *et al* PRC82(2010)

Crust and core EOS matching

Non-unified EOS

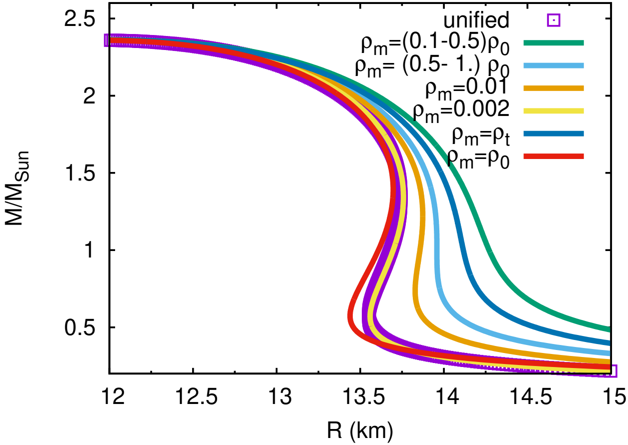

- no effect on the maximum mass
- effect on the radius of mass stars
  GM1: $\Delta R(1 M_\odot) = 0.66$km, $\Delta R(1.4 M_\odot) = 0.42$km

Crust and core EOS matching

Non-unified EOS

Building the stellar matter EOS for the TOV

- Choose an EOS for the outer crust
  - choosing BPS or RHS: almost no effect
    BPS: Baym, Pethick Sutherland ApJ 170 (1971) 299
    RHS: Ruester, Hempel, Schaffner-Bielich PRC 73 (2006) 035804
- Choose for the inner crust and EOS with similar nuclear saturation properties
- Take above crust-core transition, core EOS

Thermodynamic consistency

- $p(\mu)$ is increasing and convex
  $\rightarrow \rho = \frac{dp}{d\mu}$ is an increasing function of p

Light clusters

- Crust: matter is inhomogeneous, clusterized into nuclei.
- Above the crystallization temperature:
  - the crust melts
  - light clusters contribute to the equilibrium
- Perfect conditions for their formation:
  - core-collapse supernova environments $T \lesssim 20$ MeV
  - binary star mergers $T \lesssim 10$ MeV
- Important role in cooling neutron star, accreting systems, and binary mergers

Light clusters: setting the couplings

- Lagrangian density:

$$\mathcal{L} = \sum_{j=n,p,d,t,h,\alpha} \mathcal{L}_j + \mathcal{L}_\sigma + \mathcal{L}_\omega + \mathcal{L}_\rho + \mathcal{L}_{\omega\rho}.$$

- Tritons and helions:

$$\mathcal{L}_j = \bar{\psi}\left[\gamma_\mu i D_j^\mu - M_j^*\right]\psi,$$

- Covariant derivatives for all clusters

$$iD_j^\mu = i\partial^\mu - g_{vj}\omega^\mu - \frac{g_\rho}{2}\boldsymbol{\tau}_j \cdot \mathbf{b}^\mu,$$

$g_{vj} = A_j g_v$

Light clusters: effective mass

Pais PhysRevC.97.045805

- The total binding energy of a light cluster j

$$B_j = A_j m^* - M_j^* \,, \quad j = d, t, h, \alpha \,,$$

- Cluster effective mass:

$$M_j^* = A_j m - g_{sj}\phi_0 - \left(B_j^0 + \delta B_j\right) ,$$

- $g_{sj} = x_{sj} g_s \rightarrow$ needs to be constrained! $\rightarrow$Virial EoS
- Binding energy shift δB_j

$$\delta B_j = \frac{Z_j}{\rho_0}\left(\epsilon_p^* - m\rho_p^*\right) + \frac{N_j}{\rho_0}\left(\epsilon_n^* - m\rho_n^*\right)$$

  - the energy states occupied by the gas are excluded: double counting avoided!
  - energetic counterpart of classical exclusion volume mechanism

Cluster fractions - CLD vs HM

from Helena Pais

- CLD (heavy cluster) calculation with light clusters with and without δB_j
- Light clusters with A $\leq$ 12.

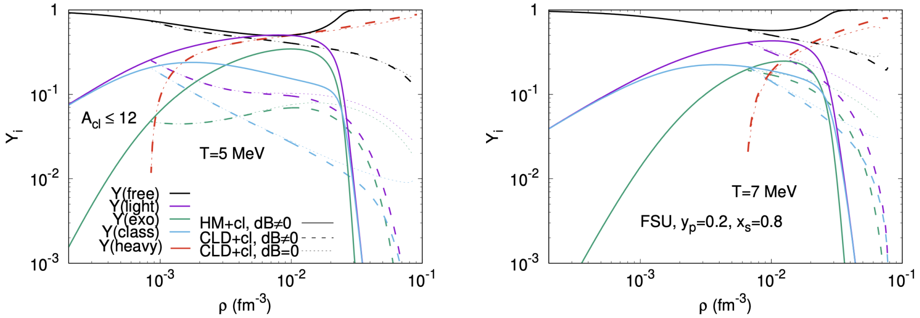

- The heavy cluster (CLD+cl calculation) makes the light clusters less abundant but increases their melting density, as compared with the HM+cl calculation.

- Increasing T makes the onset of both heavy and light clusters to increase in density.

Exp Constraint: Equilibrium constants

PRC 97, 045805 2018

- Yellow bands: exp data from Qin et al
- Red points: RMF model calculated at (T,rho,yp) of exp data with $x_s = 0.85 \pm 0.05$

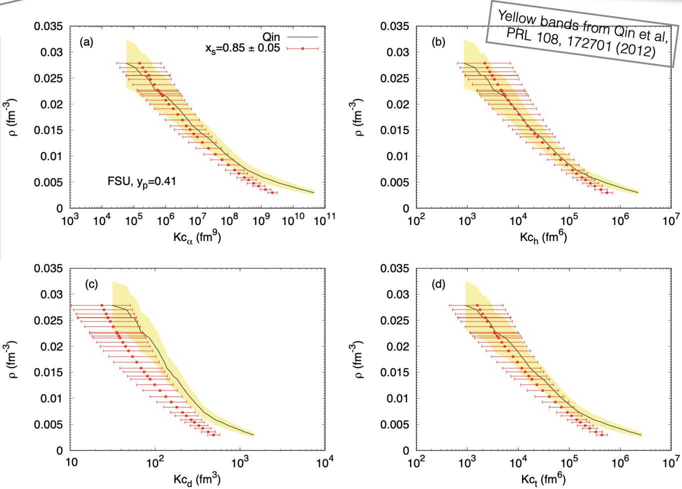

- x_s first fitted to the Virial EoS, model-ind constraint, only depends on exp B and scattering phase shifts. Provides correct zero-density limit for finite-T EoS.

- Our theoretical model describes quite well experimental data, except for deuteron

Equilibrium constants and data from INDRA

from Helena Pais

- This work shows that there are in-medium effects:
- We obtain a higher x_s as compared to the previous fit of Qin et al data:
- The higher the x_s, the bigger the binding energies (and the smaller effect of the medium), and the higher the dissolution densities of the clusters.

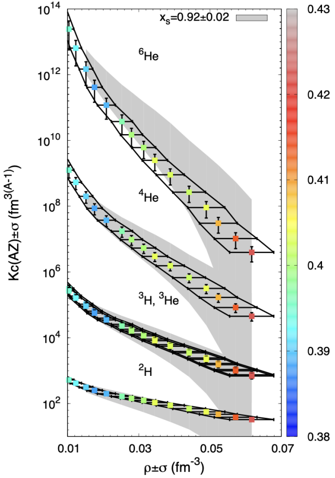

Thank you !